THE JOURNAL OF BIOLOGICAL CHEMISTRY VOL. 286, NO. 45, pp. 39297–39306, November 11, 2011

In Vivo Evidence for Epidermal Growth Factor Receptor (EGFR)-mediated Release of Prolactin from the Pituitary Gland[S]

Received for publication, March 24, 2011, and in revised form, September 12, 2011 Published, JBC Papers in Press, September 13, 2011, DOI 10.1074/jbc.M111.243493

Maik Dahlhoff[‡], Andreas Blutke[§], Rüdiger Wanke[§], Eckhard Wolf[‡], and Marlon R. Schneider[‡1]

From the [‡]Institute of Molecular Animal Breeding and Biotechnology, Gene Center, LMU Munich, Munich 81377, Germany and the [§]Institute of Veterinary Pathology, LMU Munich, Munich 80533, Germany

Background: The epidermal growth factor receptor (EGFR) regulates mammary gland development and function.
Results: Overexpression of betacellulin in transgenic mice induces a lactation-like phenotype due to increased circulating levels of prolactin.
Conclusion: The EGFR system also regulates mammary gland activity by modulating prolactin release.
Significance: We provide the first *in vivo* evidence that the EGFR system regulates prolactin release from the pituitary gland.

Members of the epidermal growth factor receptor (EGFR/ERBB) system are essential local regulators of mammary gland development and function. Emerging evidence suggests that EGFR signaling may also influence mammary gland activity indirectly by promoting the release of prolactin from the pituitary gland in a MAPK and estrogen receptor-α (ERα)-dependent manner. Here, we report that overexpression of the EGFR ligand betacellulin (BTC) causes a lactating-like phenotype in the mammary gland of virgin female mice including the major hallmarks of lactogenesis. BTC transgenic (BTC-tg) females showed reduced levels of prolactin in the pituitary gland and increased levels of the hormone in the circulation. Furthermore, treatment of BTC-tg females with bromocriptine, an inhibitor of prolactin secretion, blocked the development of the lactation-like phenotype, suggesting that it is caused by central release of prolactin rather than by local actions of BTC in the mammary gland. Introduction of the antimorphic *Egfr* allele Wa5 also blocked the appearance of the mammary gland alterations, revealing that the phenotype is EGFR-dependent. We detected an increase in MAPK activity, but unchanged phosphorylation of ERα in the pituitary gland of BTC-tg females as compared with control mice. These results provide the first functional evidence *in vivo* for a role of the EGFR system in regulating mammary gland activity by modulating prolactin release from the pituitary gland.

Mammary gland development takes place essentially in the postnatal period under the influence of systemic hormones and locally synthesized growth factors. Prolactin, a polypeptide hormone synthesized in the anterior pituitary gland, is a major systemic regulator of mammary gland function, orchestrating lobualveolar differentiation at puberty (mammogenesis), milk production at the end of pregnancy (lactogenesis), and maintenance of milk secretion (galactopoiesis) (1–3). Upon binding to its cognate receptor in mammary gland cells, prolactin promotes the phosphorylation of the nonreceptor tyrosine kinase Janus kinase 2 (JAK2) (4). JAK2 initiates multiple downstream signaling pathways, including the signal transducer and activator of transcription (STAT)[2] pathway. Activation (phosphorylation), dimerization, and nuclear translocation of STAT5 mediate the majority of prolactin-induced differentiation of mammary epithelial cells during pregnancy and lactation (5, 6).

There is ample evidence that the epidermal growth factor receptor (EGFR/ERBB1) system, including the four tyrosine kinase receptors ERBB1 to ERBB4 (7) and seven ligands (8), is a major local regulator of mammary gland activity. First, the four receptors and most ligands were shown to have a distinct, specific expression pattern in the virgin, pregnant, lactating, and involuting mammary gland (9). Second, introduction of recombinant protein or retroviral expression of the EGFR ligands EGF, transforming growth factor-α (TGFA), and amphiregulin (AREG) induced ductal morphogenesis and lobular hyperplasia in the mouse mammary gland (10, 11). Third, the phenotype of mice lacking individual receptors strongly suggest that each ERBB family member regulates different aspects of mammary gland development (reviewed in Refs. 12, 13). For example, ERBB4 is required for STAT5 phosphorylation, and loss of ERBB4 activity results in impaired mammary gland differentiation (14–16). Among the EGFR ligands, AREG appears to be the most important one because its loss impairs mammary gland development (17). Mechanistically, AREG is an essential mediator of estrogen receptor α (ERα) actions during puberty-induced ductal elongation, but dispensable for any earlier or later developmental stages of the mammary gland (18).

In addition to this extensive, well documented local role of the EGFR system in the mammary gland, emerging evidence suggests that its members may influence mammary gland

[S] The on-line version of this article (available at http://www.jbc.org) contains supplemental Fig. S1.

[1] To whom correspondence should be addressed: Institute of Molecular Animal Breeding and Biotechnology, Gene Center, LMU Munich, Feodor-Lynen-Str. 25, 81377 Munich, Germany. Tel.: 49-89-218076815; Fax: 49-89-218076849; E-mail: schnder@lmb.uni-muenchen.de.

[2] The abbreviations used are: STAT, signal transducer and activator of transcription; EGFR, epidermal growth factor receptor, BTC, betacellulin; BTC-tg, BTC transgenic; AREG, amphiregulin; TEB, terminal end bud; TUB, tubulin.

development indirectly by altering the expression and/or release of prolactin from the pituitary gland. It has been long known that lactotrophs express the EGFR and several of its ligands (19, 20) and that EGF can stimulate transcription of the prolactin gene (21). In this regard, the EGFR behaves similarly to recognized stimulators of prolactin release such as the thyrotropin-releasing hormone (22) and estrogen (23). Recently, Kansra and co-workers (24) showed that, at least in cultured GH3 lactotrophs, EGF-induced prolactin expression and release are mediated by the ERα. However, the *in vivo* relevance of these findings remains to be demonstrated. In this report, we present data supporting the ability of the EGFR system to induce prolactin release from the pituitary gland *in vivo*.

EXPERIMENTAL PROCEDURES

Animals and in Vivo Experiments—Animals were maintained under specific pathogen-free conditions at 23 °C, 65% humidity and with 12-h light/dark cycle and had free access to a standard rodent diet (V1534, Ssniff, Soest, Germany) and water. All animal experiments were carried out in accordance with the German Animal Welfare Act with permission from the responsible veterinary authority. Two different transgenic mouse lines overexpressing betacellulin were generated via pronuclear DNA microinjection into zygotes from the inbred strain FVB/N and were previously described in detail (25). Wa5 mice on the C57BL/6N background carrying an antimorphic *Egfr* allele were donated by the Medical Research Council (Oxford, UK) via Dr. David Threadgill. Bromocriptine (10 mg/kg) (Sigma-Aldrich) was diluted in saline/water/ethanol (60/20/20) and bromocriptine or vehicle was administered daily by intraperitoneal injection over 11 weeks.

Quantitative RT-PCR—Mammary gland and pituitary gland tissue was homogenized in TRIZOL® (Invitrogen, Karlsruhe, Germany) for RNA isolation. 5 μg of RNA samples were reverse-transcribed in a final volume of 35 μl using Superscript™ II Reverse Transcriptase (Invitrogen, Karlsruhe, Germany) according to the manufacturer's instructions. Quantitative mRNA expression analysis was performed by real-time quantitative reverse-transcription polymerase chain reaction (qRT-PCR) using the LightCycler® 480 System (Roche, Mannheim, Germany). Final primer concentration was 0.5 μM and probe concentration was 0.2 μM. LightCycler® 480 Probes Master were used, the final reaction volume was 20 μl, and cycle conditions were 95 °C for 5 min for the first cycle, followed by 45 cycles of 95 °C for 10 s, 60 °C for 15 s, and 72 °C for 1 s. Quantitative values are obtained from the Ct number at which the increase in the signal associated with the exponential growth of PCR products begins to be detected. Transcript copy numbers were normalized to *Actb* mRNA copies. Results are expressed as fold differences in *Prl* gene expression relative to *Actb* transcripts. The ΔCt value of the sample was determined by subtracting the average Ct value of the target gene from the average Ct value of the *Actb* gene. TaqMan primers and probes for *Prl* cDNA (Thermo Fisher Scientific, Ulm, Germany) were designed to span exon junctions or to lie in different exons to prevent amplification of genomic DNA. Their sequences were as follows: forward primer 5′-GGGTCAGCCCAGAAAGCAG-3′; reverse primer 5′-CAGTCACCAGCGGAACAGATT-3′; fluorogenic probe 5′-CTGCTGTTCTGCCAAAATGTTCAGCCTCT-3′. Probes were labeled with the reporter dye FAM at the 5′ and the quencher dye TAMRA at the 3′-end. *Actb* primer and probe sequences were: forward primer 5′-CGTGAAAAGATGACCCAGATCA-3′; reverse primer 5′-CACAGCCTGGATGGCTACGT-3′; fluorogenic probe 5′-TTTGAGACCTTCAACACCCCAGCCA-3′. For each primer pair we performed no-template control and no-RT control assays, which produced negligible signals that were usually greater than 40 in Ct value. Experiments were performed in duplicates for each sample.

Western Blot Analysis—Western blot experiments have been described in detail before (26). Briefly, samples were homogenized in extraction buffer and equal amounts of protein were electrophoresed on 12% polyacrylamide-sodium dodecyl sulfate gels and then blotted to PVDF-membranes (GE Healthcare, Munich, Germany). Incubation with primary antibodies was carried out overnight at 4 °C. Following antibodies (diluted in 5% dry milk) were used: goat anti-prolactin (1:500; #sc-7807; Santa Cruz Biotechnology), goat anti-betacellulin (1:500; #AF1025; R&D Systems), rabbit anti-phospho-p44/42 MAPK (Thr 202/Tyr 204; 1:2000; #9101; Cell Signaling), rabbit anti-p44/42 MAPK (1:2000; #9102; Cell Signaling), rabbit anti-phospho-STAT5 (1:2000; #9359; Cell Signaling), rabbit anti-STAT5 (1:2000; #9358; Cell Signaling), mouse anti-estrogen receptor α (1:1000; #2512; Cell Signaling), mouse anti-phospho-estrogen receptor α (Ser-118) (1:1000; #2511; Cell Signaling), rabbit anti-phospho-estrogen receptor α (Ser-104/106) (1:1000; #2517; Cell Signaling), rabbit anti-phospho-estrogen receptor α (Ser167) (1:1000; #5587; Cell Signaling), rabbit anti-GAPDH (1:5000; #2118; Cell Signaling), rabbit anti-α-tubulin (1:5000; #2125; Cell Signaling). Appropriate horseradish peroxidase-conjugated secondary antibodies were used. Immunoreactive bands were visualized by chemiluminescence with ECL kit (GE Healthcare). Band intensities were quantified using the ImageQuant software package (GE Healthcare). For measurement of kinases and transcription factor activities bands were analyzed densitometrically followed by normalization to the corresponding total α-tubulin or GAPDH signals.

Whole Mount Preparation, Histology, Morphometric, and Quantitative Stereological Analyses of the Mammary Gland—Mammary gland development and morphology were studied in histological sections, and in whole mount preparations of the fourth abdominal mammary gland. For whole mount preparations, mammary gland complexes were mounted on slides, fixed overnight, stained with carmine alum (Sigma), defatted, clarified, and mounted with Eukitt® (Sigma), as described earlier (18). Histological analyses were performed on hematoxylin and eosin (H&E)-stained paraffin sections of paraformaldehyde-fixed (4%) mammary glands. Mammary gland morphology of control mice and of heterozygous BTC-tg animals was analyzed in histological sections ($n = 3$ for each group per investigated age), and in whole mount mammary gland preparations from mice at four (2/2), six (3/4) and eight (3/4) weeks and five months (4/2) of age. Images of whole mount preparations were acquired using a digital camera (Olympus DP72) attached to a microscope (Olympus BX41). Morphometric analyses of duct length, ductal branching, and numbers and

sizes of buds were performed on whole mount mammary gland preparations from three control and three BTC-tg mice at 6 and at 8 weeks of age, and from three Wa5 mice at 8 weeks of age, using a Videoplan image analysis system (Zeiss-Kontron, Munich, Germany). The lengths of ducts in the mammary fat pad were measured along their longitudinal axis, using a 25× magnification. In addition to the total duct length (including primary, secondary, and tertiary ducts, terminal end buds, side buds, alveolar buds, and alveoli), the lengths of primary ducts were measured separately. The numbers of buds and alveoli (subdivided into terminal end buds (TEBs), side buds and alveolar buds and alveoli), and the numbers of branch points along the ductal network, subdivided into primary branches, secondary branches and total number of branches (including primary, secondary and tertiary branches, and diverging side buds and alveolar buds) were counted (magnification 25×). For estimation of ductal branch density, the numbers of the respective branch points per 1 mm of duct length were calculated. In digital images of whole mount preparations, the total area of ducts, buds and alveoli, and the total area of the mammary gland fat pad were determined by point counting (863 ± 322 points per case). The relative outgrowth area of ducts, buds and alveoli in the mammary gland was calculated as the quotient of these areas. To characterize the size of single alveoli, the mean areas of single alveoli or alveolar buds were determined. For this, the areas of 84 ± 14 single alveoli per case were measured planimetrically inside each of ten systematically randomly sampled test fields (magnification 100×) in whole mount mammary gland preparations. Mammary gland morphology of Wa5, BTC-tg/Wa5 double transgenic mice, BTC-tg mice, and control mice was studied in whole mount preparations at 8 weeks (n = 3/2/3/3), and in whole mount preparations and histological sections at 12 months of age (3/4/2/3). For quantitative stereological investigations of the mammary gland of 14 weeks old bromocriptine-treated BTC-tg mice (BTC-tg +B, n = 5), bromocriptine-treated controls (Control +B, n = 4), BTC-tg mice (n = 3), and untreated control mice (n = 3), the mammary gland complexes were fixed in 4% paraformaldehyde routinely embedded in paraffin and completely cut into consecutive sections of ~3 μm thickness. Per case, every 90th-240th section (13 ± 3 equidistant sections per case) was selected and stained with HE. The fractional volumes (volume densities, V_V) of the mammary epithelial parenchyma (lactiferous ducts, alveolar buds, lobules, and acini) in the mammary gland ($V_{V(\text{mammary epithelial parenchyma/mammary gland})}$) were determined by point counting (10264 ± 2020 points per case) in systematically randomly selected areas (116 ± 22 per case), using an automated stereology system (VIS-Visiopharm Integrator System® Version 3.4.1.0 with newCAST® software, Visiopharm A/S, Hørsholm, Denmark) (27).

Immunohistochemistry—For immunohistochemistry, tissues were fixed, deparaffinized, rehydrated, and boiled for antigen retrieval for 20 min in 10 mM citrate buffer pH 6.0. After blocking, the sections were incubated with prolactin-, betacellulin-, phospho-STAT5 or STAT5-antibody (see "Western blot" section) and Ki67 (Dako, Hamburg, Germany) overnight at 4 °C. After incubation with a secondary biotin-conjugated antibody and a tertiary complex of streptavidin-biotin the sections were stained with 3,3′-diaminobenzidine (KEN-EN-TEC, Taastrup, Denmark) and counterstained with Mayer's hematoxylin.

Quantitative Analysis of Cell Proliferation—To determine the percentage of Ki67 positive nuclei, the number of Ki67-positive nuclei and the total nuclei number in ducts, buds and alveoli present in a section of the fourth abdominal mammary gland were counted (n = 3 mice/group). For the 6 weeks group, the mean total number of cells counted was 836 ± 9 (control) and 1426 ± 160 (BTC-tg); for the 5 months group, the numbers were 465 ± 33 (control) and 405 ± 36 (BTC-tg).

Determination of Circulating Prolactin Levels—Serum prolactin levels shown in Fig. 4*D* were determined with an enzyme-linked immunosorbent assay (ELISA) from USCN Life Science Inc. (China). A second ELISA kit was employed to determine the serum prolactin levels shown in Fig. 5*C* (Cusabio Biotech CO., LTD, Japan).

Statistical Analysis—Data of quantitative stereological investigations were analyzed by analysis of variance, taking the effects of genetic group and bromocriptine treatment into account. Means were compared by using Bonferroni post hoc tests (SPSS program package; SPSS, Chicago, USA). $p < 0.05$ was considered significant. Two tailed Student's t-tests were used for analysis of the other data sets. Data are presented as means ± S.D. Group difference were considered to be statistically significant if $p < 0.05$.

RESULTS

Virgin BTC-tg Females Show a Lactation-like Phenotype—A morphological alteration of the mammary gland consisting of brownish color and an apparent increase in tissue hardness was observed during routine necropsy of adult, virgin BTC-tg females (Fig. 1*A*). This alteration was observed in two independent transgenic lines, but all further experiments were performed with virgin females from line 2. Both the absolute and the relative weight of the organ were significantly reduced in BTC-tg females as compared with control littermates (Fig. 1*B*). To gain more insight into the alteration, analysis of whole mount preparations and histological analysis were carried out. Mammary glands of control and BTC-tg mice at 4 weeks of age were characterized by the formation of few branched lactiferous ducts with terminal end buds invading the mammary fat pad (Fig. 1*C* and Fig. 2, *first row*) (28). However, BTC-overexpressing females exhibited a strong hyperplastic growth effect on the epithelial mammary parenchyma in the mammary gland, starting at 6 weeks of age. The total duct lengths in the mammary glands of BTC-tg mice were significantly increased, and their lactiferous duct system showed a more complex branching pattern with significantly increased numbers of branches, as compared with controls (Fig. 1*C* and Fig. 2, *second row*; Table 1), indicating an accelerated mammary gland development of BTC-tg mice at this time point.

From 6 weeks of age onwards, the mammary gland phenotype of BTC-tg mice was primarily characterized by significantly augmented and progressively increasing relative outgrowth areas of ducts, buds and alveoli in the mammary gland, along with significantly elevated numbers and sizes of alveoli and alveolar buds (Table 1), as compared with age matched

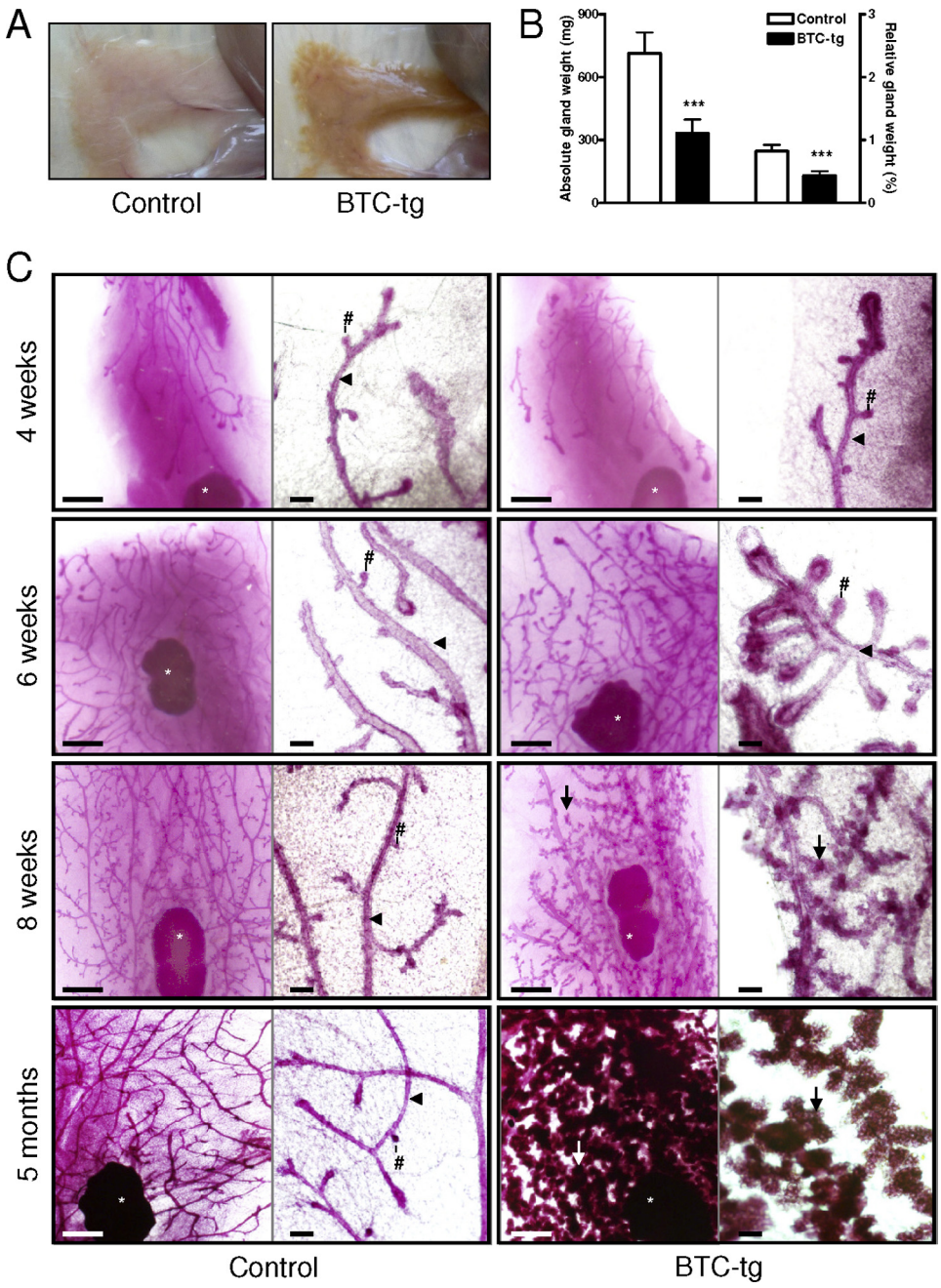

FIGURE 1. Macroscopical aspect (*A*) and absolute and relative weights (*B*) of the mammary gland of BTC-tg females and control littermates at the age of 5 months. Whole mount preparations (*C*) of 4th abdominal mammary gland complexes of control mice (*left columns*) and BTC-tg females (*right columns*) at 4, 6, and 8 weeks, and at 5 months of age. Per genotype and age, a survey view (*left*, bar = 1 mm) and a higher magnification (*right*, bar = 100 μm) are shown. Lymph nodes (*white asterisks*), lactiferous ducts (*arrowheads*), end/side buds (#), alveolar buds, lobules and acini (*arrows*) are indicated. Note the increased formation of alveolar buds, lobules, and acini in BTC-tg mice from 6 weeks of age onwards. Means ± S.D., ***: $p < 0.001$.

controls. At 8 weeks of age, several large alveolar lobules, flanking the lactiferous ducts in the mammary glands of BTC-tg mice had developed (Fig. 1*C* and Fig. 2, *third row*), and the significantly augmented relative outgrowth areas of ducts, buds, and alveoli in the mammary gland, as well as the numbers and sizes of alveoli and alveolar buds in BTC-tg mice had further increased. However, the differences in duct lengths and ductal branching patterns between BTC-tg and control mice were almost equalized at 8 weeks of age (Table 1). At five months of age, the alveolar acini had filled the majority of the mammary gland fat pad in BTC-tg mice (Fig. 1*C* and Fig. 2, *fourth row*). The alveolar epithelial cells displayed a vacuolated cytoplasm, and a milk-like secretion with protein and lipid droplets was present in the luminar spaces of the acini and lactiferous ducts of BTC-tg mice (Fig. 2, *fourth row*).

Immunohistochemistry against Ki67 showed that the morphological alterations of the mammary gland in BTC-tg females were accompanied by increased cell proliferation at the age of 6 weeks, which was also present at 5 months of age (supplemental Fig. 1*A*). Quantitative analysis confirmed a significant increase in cell proliferation at these ages (supplemental Fig. 1*B*). Phosphorylation of STAT5, a key event for the mammary epithelial

differentiation program, was absent in the mammary gland of young (4 weeks old) BTC-tg females and control littermates but clearly present in adult (5 months) BTC-tg glands as shown by Western blot (supplemental Fig. 1*C*) and immunohistochemical analysis (supplemental Fig. 1*D*).

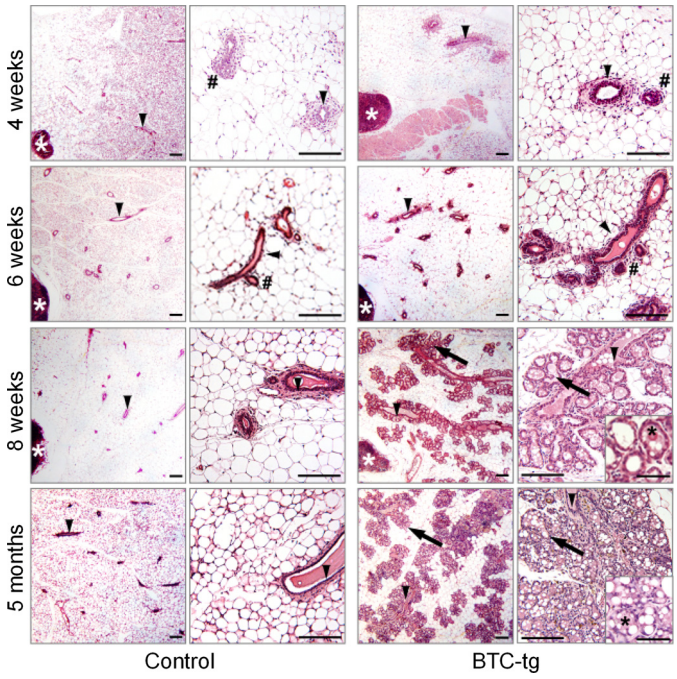

FIGURE 2. **Histology of mammary gland development in non-transgenic control mice (*left column*) and BTC-tg mice (*right column*) at 4, 6, and 8 weeks, and at 5 months of age.** Per genotype and age, a survey view (*left*, bar = 200 μm) and a higher magnification (*right*, bar = 100 μm) are shown. The histology of alveolar epithelial cells of BTC-tg mice is shown in inset pictures for BTC-tg mice at 8 weeks and 5 months of age (bar = 50 μm). Lymph nodes (*white asterisks*), lactiferous ducts (*arrowheads*), end/side buds (#), alveolar lobules and acini (*arrows*), and milk-like secretion (*black asterisks*) are indicated. Paraffin sections of the fourth abdominal mammary gland complexes, H&E staining.

Next, we evaluated whether increased levels of BTC could be detected in the mammary gland and in the pituitary gland, the source of prolactin, the main hormonal regulator of lactation. The presence of BTC was readily detected by Western blot analysis in the mammary gland of BTC-tg females in contrast to control females (Fig. 3*A*), and immunohistochemistry showed that the glandular epithelium of BTC-tg mice was rich in BTC (Fig. 3*B*). Interestingly, while BTC was present in only a few pituitary cells in control mice (Fig. 3*D*, *arrows*) large amounts of BTC were evident in the pituitary gland of BTC-tg females (Fig. 3, *C* and *D*), raising the question of whether the lactation-like phenotype is a local effect of increased BTC levels in the mammary gland or a consequence of increased prolactin synthesis or release from the pituitary gland.

BTC Increases the Release of Prolactin from the Pituitary Gland without Altering Its Expression—To evaluate if BTC altered the expression of prolactin in the pituitary gland, we evaluated the *Prl* mRNA levels by quantitative RT-PCR. As shown in Fig. 4A, there were no differences in *Prl* expression between BTC-tg and control mice. In contrast, protein levels of prolactin were significantly reduced in the pituitary glands of BTC-tg females compared with control females as shown by Western blot (Fig. 4*B*) and immunohistochemistry (Fig. 4*C*). The reduction in pituitary prolactin levels was accompanied by an increase in circulating prolactin levels (Fig. 4*D*). Western blot analysis also showed presence of prolactin in the mammary tissue of BTC-tg females at the age of 5 and 9 months (Fig. 4*E*). However, prolactin mRNA levels were not altered (Fig. 4*F*), indicating that the detected prolactin protein is derived from the circulation. Collectively, these data suggest that BTC, while not influencing the expression of prolactin in the pituitary of mammary glands, promotes its release from the pituitary gland resulting in increased circulating and local (mammary gland) levels of the hormone.

TABLE 1

Morphometric analysis of mammary gland development in whole mount preparations of BTC- tg and control mice

The mammary gland phenotype of BTC-tg mice was characterized by significantly augmented relative outgrowth areas of ducts, buds, and alveoli in the mammary gland, due to increased numbers and sizes of alveoli and alveolar buds at 6 and at 8 weeks of age. Compared to controls, mammary gland development of BTC-tg mice was accelerated, with significantly increased duct lengths and numbers of branches at 6 weeks of age, whereas at 8 weeks of age, duct length, and branching patterns were almost equalized between BTC-tg mice and controls.

Morphometric parameter	Investigated ages and genotypes			
	6 weeks		8 weeks	
	Control	BTC-tg	Control	BTC-tg
Relative outgrowth area of ducts, buds and alveoli in the mammary gland	0.05 ± 0.01	0.17 ± 0.04[a]	0.05 ± 0.02	0.20 ± 0.02[a]
Duct length				
Total duct length (mm)	218 ± 20.9	329 ± 29.3[a]	427 ± 119.7	367 ± 47.8[b]
Length of primary ducts (mm)	113 ± 46.2	199 ± 41.5[b]	253 ± 45.2	208 ± 21.1[b]
Branches				
Total number of branches	209 ± 37.2	431 ± 81.8[a]	587 ± 184	675 ± 171[b]
Primary branches	53.3 ± 24.8	97.7 ± 13.0[b]	100 ± 19.1	101 ± 96.1[b]
Secondary branches	106 ± 41.2	279 ± 27.3[a]	421 ± 145	489 ± 96.1[b]
Total number of branches per mm total duct length	0.95 ± 0.10	1.31 ± 0.18[c]	1.38 ± 0.32	1.85 ± 0.53[b]
Primary branches per mm length of primary ducts	0.47 ± 0.09	0.50 ± 0.08[b]	0.40 ± 0.09	0.48 ± 0.06[b]
Secondary branches per mm length of primary ducts	0.95 ± 0.10	1.42 ± 0.16[a]	1.63 ± 0.30	2.36 ± 0.55[b]
Alveoli and buds				
Number of terminal end buds	17.7 ± 2.5	15.3 ± 9.1[b]	10.7 ± 10.8	11.0 ± 9.5[b]
Number of alveolar buds and side buds	146 ± 29.9	479 ± 65.3[d]	787 ± 278	1430 ± 483[c]
Mean area of single alveoli in whole mounts (μm^2)	723 ± 83	2196 ± 228[d]	1084 ± 318	2469 ± 426[c]

[a] Significance of differences within a parameter between age-matched BTC-tg and control mice: $p < 0.01$.
[b] ns, not significant.
[c] $p < 0.05$.
[d] $p < 0.001$.

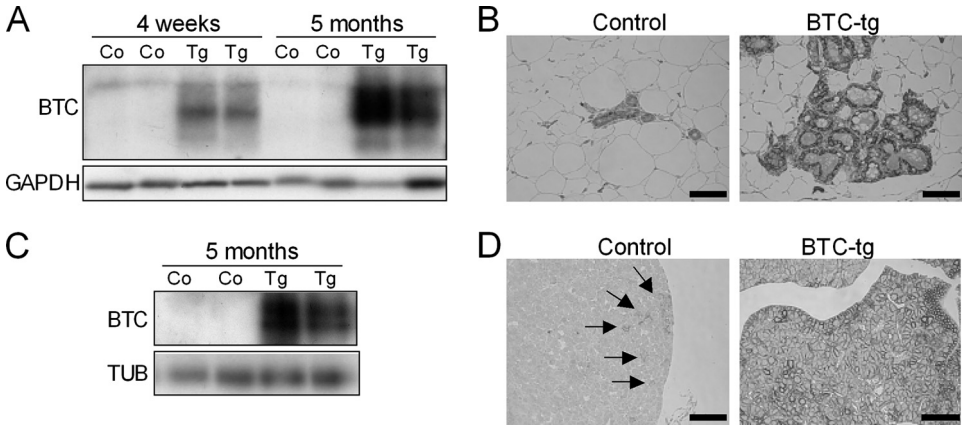

FIGURE 3. **Increased levels of BTC were detected in the mammary gland (*A* and *B*) and in the pituitary gland (*C* and *D*) by Western blot analysis (*A* and *C*) and immunohistochemistry (*B* and *D*).** *Arrows* indicate BTC-positive cells in the pituitary of control females. Bars correspond to 50 μm.

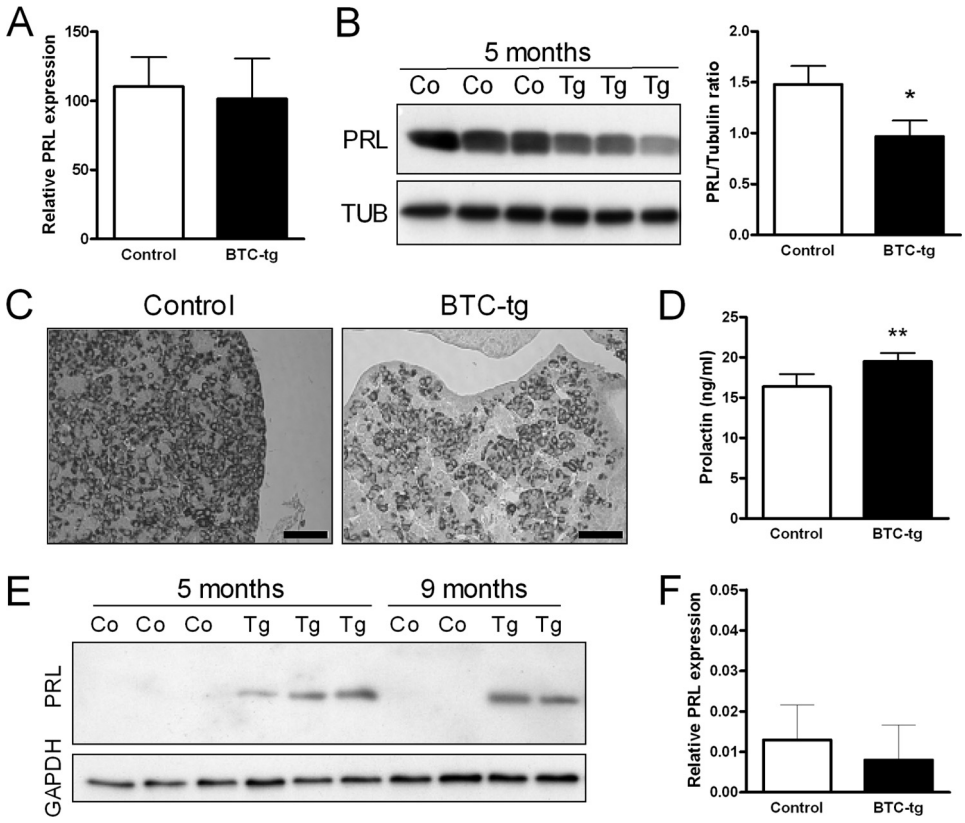

FIGURE 4. Prolactin mRNA levels are unchanged in the pituitary gland of BTC-tg mice as compared with control females (*A*). In contrast, less prolactin protein is detectable in the pituitary of BTC-tg females by Western blot analysis (*B*) and immunohistochemistry (*C*). Serum prolactin levels are significantly increased in BTC-tg females as compared with control mice (*D*). Prolactin protein is detectable in mammary gland tissue extracts of BTC-tg females at 5 and 9 months of age but not in control females (*E*). Prolactin mRNA levels are not increased in the mammary gland of BTC-tg females (*F*). If not otherwise indicated, mice were at 5 months of age. Bars correspond to 50 μm. Means $\pm$ S.D., *: $p < 0.05$; **: $p < 0.01$.

Inhibition of Prolactin Release Completely Reverts the Mammary Gland Phenotype of BTC-tg Mice—To evaluate to which extent the increased circulating levels of prolactin are responsible for the lactation-like phenotype in the mammary glands of BTC-tg females, we treated 3 weeks old transgenic and control females with bromocriptine, an inhibitor of prolactin secretion, for 11 weeks. At the end of the experiment, the fourth abdominal mammary gland complexes were collected and the volume density of the mammary epithelial parenchyma (lactiferous ducts, alveolar buds, lobules, and acini) ($V_{V(\text{mammary epithelial parenchyma/mammary gland})}$) was determined by stereological techniques. Bromocriptine treatment did not cause a noticeable effect on the morphology of the mammary gland of control mice. In BTC-tg mice, however, bromocriptine treatment nearly completely abolished the BTC-induced hyperplastic growth effects of alveolar lobules observed in the mammary gland (Fig. 5*A*). These findings were confirmed by quantitative stereological analyses of the tissue composition of the mammary gland of control mice, BTC-tg mice, bromocriptine-treated controls, and bromocriptine-treated BTC-tg mice. The $V_{V(\text{mammary epithelial parenchyma/mammary gland})}$ of BTC-tg mice was significantly increased as compared with control mice. Bro-

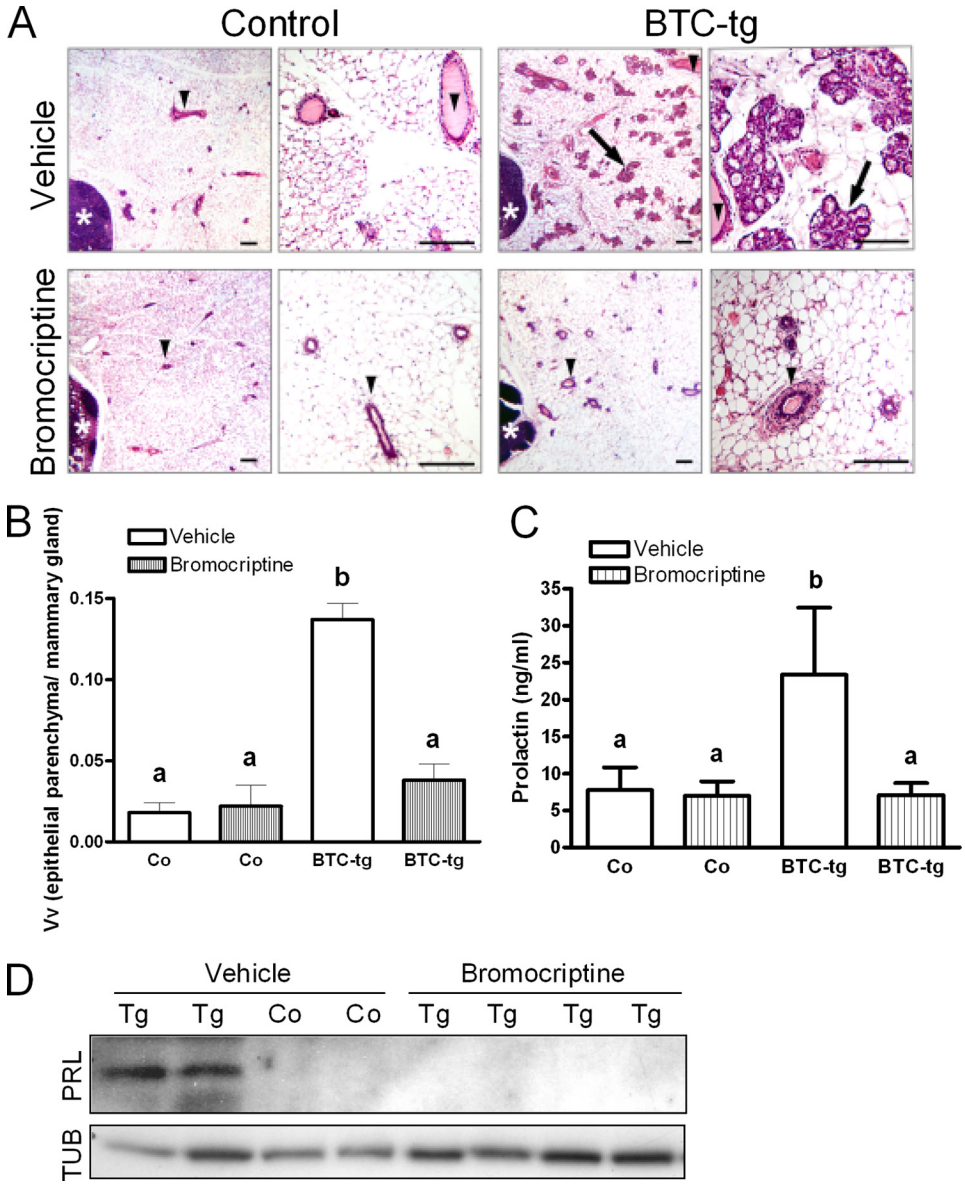

FIGURE 5. *A*, histology of the fourth abdominal mammary gland complex of control females and BTC-tg females treated with vehicle (*upper panels*) or bromocriptine (*lower panels*) for 11 weeks. Per genotype, a survey view (*left*, bar = 200 μm) and a higher magnification (*right*, bar = 100 μm) are shown. Lymph nodes (*white asterisks*), lactiferous ducts (*arrowheads*), alveolar lobules (*arrows*). Paraffin sections, H&E staining. *B*, volume densities of mammary epithelial parenchyma (lactiferous ducts, alveolar buds, lobules, and acini) in the mammary gland ($V_{V(\text{mammary epithelial parenchyma/mammary gland})}$) of the same animals ($n$ = 3–5/group). *C*, while bromocriptine treatment did not alter serum prolactin levels in control mice, it significantly reduced the serum levels of the hormone in BTC-tg mice (same animals as above). *D*, Western blot analysis showing that bromocriptine treatment abolished the occurrence of prolactin (*PRL*) in the mammary glands of BTC-tg females. *TUB*: tubulin. Data in *B* and *C* are means ± S.D. Significant differences (*B*: $p < 0.001$, *C*: $p < 0.01$) between the respective groups are indicated by different superscripts (a, b).

mocriptine treatment of BTC-tg mice significantly reduced the volume density of the mammary epithelial parenchyma in the mammary gland to the level of control mice or bromocriptine treated control mice (Fig. 5*B*). While bromocriptine treatment did not alter serum prolactin levels in control mice, it significantly reduced the serum levels of the hormone in BTC-tg mice (Fig. 5*C*). Finally, Western blot analysis showed that bromocriptine treatment abolished the occurrence of prolactin (PRL) in the mammary glands of BTC-tg females (Fig. 5*D*). Thus, treatment of BTC-tg mice with bromocriptine completely prevented the formation of the lactation-like phenotype, indicating that the phenotype is a consequence of increased prolactin release from the pituitary gland.

The Lactation-like Phenotype Is Mediated by the EGFR—Wa5 mice carry an antimorphic *Egfr* allele resulting in significantly blunted EGFR activity (29). Analysis of whole mount preparations and histological evaluation of mammary glands of Wa5 mice and control mice at 8 weeks (Fig. 6, *upper panel*), and at one year (Fig. 6, *lower panel*) of age did not reveal conspicuous morphological differences. Morphometric analysis of mammary glands of 8 weeks old Wa5 mice and control mice did not reveal significant differences in the relative outgrowth area of mammary gland epithelial parenchyma in the mammary gland, total duct length, total number of branches, the mean area of single alveoli, number of TEBs, or number of alveolar buds and side buds (data not shown), although a strong tend-

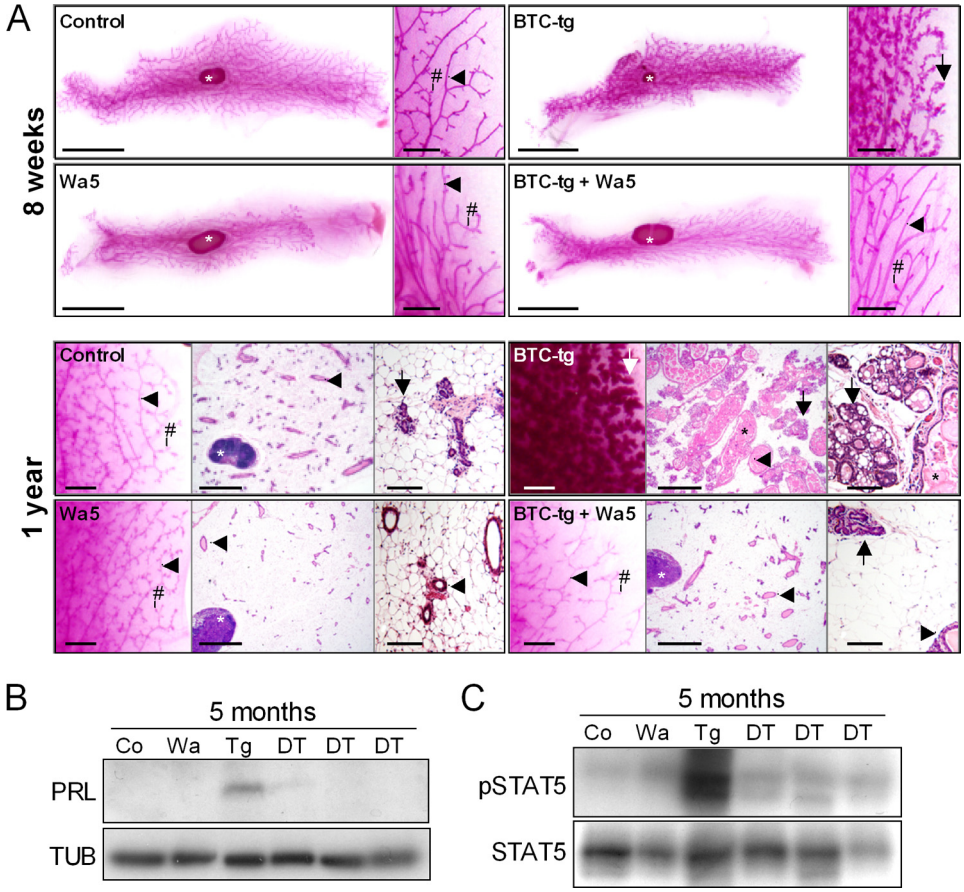

FIGURE 6. *A*, mammary gland morphology (4th abdominal mammary gland complexes) of control, BTC-tg, Wa5 and BTC/Wa5 double-transgenic mice. *Top panel*, mammary gland whole mount preparations of 8 weeks old mice. Per genotype, a survey view (*left*, bar = 1 cm) and a higher magnification (*right*, bar = 1 mm) are shown. *Bottom panel*: whole mount preparations and histology (paraffin sections, H&E staining) of mammary glands of 1-year-old mice. Per genotype, a higher magnification of a whole mount preparation (*right*, bar = 1 mm), a survey view of a histological section (*middle*, bar = 1 mm) and a higher magnification of a histological section (*right*, bar = 100 μm) are shown. Lymph nodes (*white asterisks*), lactiferous ducts (*arrowheads*), side buds (#), alveolar buds, lobules, and acini (*arrows*), and milk-like secretion (*black asterisks*) are indicated. Note the reduction of hyperplastic growth of alveolar acini in BTC/Wa5-tg mice as compared with BTC-tg mice. *B*, Western blot showing that the presence of prolactin in the mammary gland, visible in BTC-tg females, disappears after crossing into the EGFR dominant-negative background Wa5 (*DT*, double transgenic mice). *C*, Western blot showing the disappearance of phosphorylated STAT5 in the mammary gland of BTC-tg females after crossing into the EGFR dominant-negative background Wa5 (*DT*, double transgenic mice).

ency to reduced numbers of alveolar buds and side buds in Wa5 mice was detected (Wa5: 388 ± 150 *versus* control: 787 ± 278). Importantly, in the mammary glands of BTC/Wa5-double transgenic mice, the hyperplastic growth of alveolar acini present in BTC-tg mice was almost entirely absent, and only few numbers of small clusters of alveolar buds with flattened epithelial cells were present (Fig. 6*A*). Furthermore, both the prolactin and the phosphorylated STAT5 present in the mammary gland of BTC-tg females as detected by Western blot analysis disappeared in BTC/Wa5 double transgenic mice (Fig. 6, *B* and *C*), supporting the concept that BTC causes the described changes by activating the EGFR instead of other ERBBs in pituitary lactotrophs.

Activation of the MAPK Pathway but Not of the ERα in the Pituitary Gland of BTC-tg Females—Because it has been recently shown that EGF induces prolactin expression and release by a MAPK-mediated phosphorylation of Ser-118 on the ERα of cultured lactotrophs (24), we evaluated a possible activation of these molecules in the pituitary gland of BTC-tg mice. As shown in Fig. 7A, the MAPK pathway was strongly activated in the pituitary samples from BTC-tg females as compared with control littermates. However, Western blot analysis (Fig. 7*B*) and its densitometric evaluation (Fig. 7*C*) did not reveal a difference in the phosphorylation of Ser-104/106, Ser-118, or Ser-167 on the ERα between groups.

DISCUSSION

Members of the EGFR/ERBB family are recognized local regulators of mammary gland development and function (see Introduction). In addition to this established local role of the EGFR system, it has been suggested that its members may also influence mammary gland activity indirectly by altering the expression and/or release of prolactin from the pituitary gland. However, so far available evidence is restricted to the expression of the EGFR and several of its ligands in lactotrophs (19, 20), and to *in vitro* data showing that EGF can induce prolactin expression and release from the pituitary gland (21, 24).

In this study, we provide for the first time *in vivo* evidence that activation of the EGFR in lactotrophs can induce release of prolactin from the pituitary gland into the circulation, resulting in a lactation-like phenotype in the mammary gland. This phenotype integrated the major hallmarks of lactogenesis, including growth of the mammary epithelial parenchyma (increased numbers of alveolar and side buds and increased alveoli area),

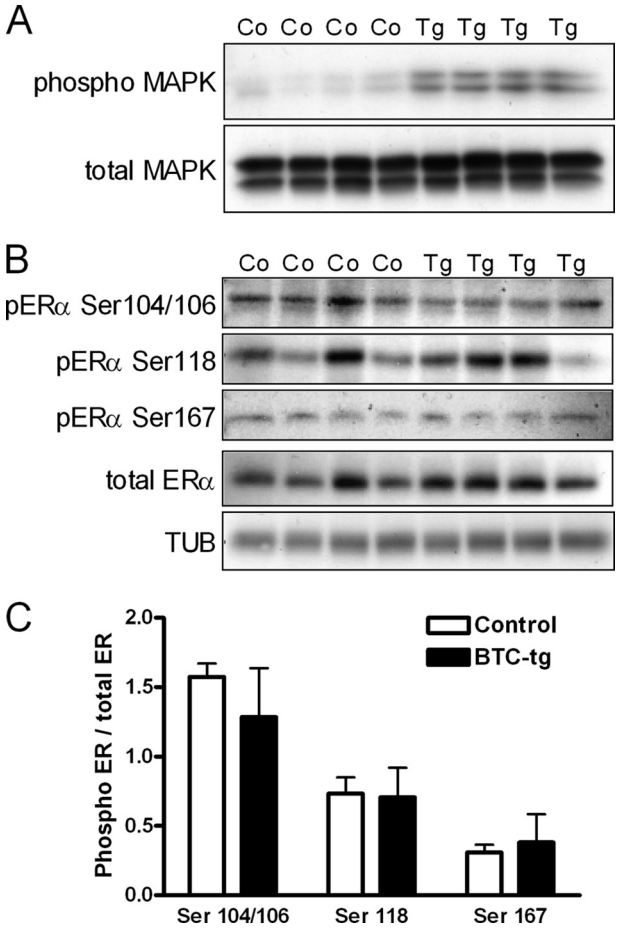

FIGURE 7. *A*, increased activation of the MAPK pathway in the pituitary glands of 8-week-old BTC-tg females as compared with control littermates. *B*, Western blot analysis of the phosphorylation of Ser-104/106, Ser-118, or Ser-167 on the ERα, total ERα, and TUB in the pituitary glands of BTC-tg females as compared with control littermates (same animals as in *A*). *C*, densitometric analysis of the data shown in *B* revealed no differences in the phosphorylation of Ser-104/106, Ser-118, or Ser-167 on the ERα in pituitary cells between groups.

phosphorylation of STAT5, and the presence of a milk-like secretion with proteins and lipid droplets in the luminar spaces of the acini and lactiferous ducts. Our studies initiated with the fortuitous observation of macroscopically visible changes in the mammary gland of transgenic females overexpressing the EGFR ligand betacellulin (25). The increased solidness and the reduced weight of the mammary glands from BTC-tg females can be attributed to the replacement of fat by mammary epithelial parenchyma. After characterizing the changes in whole mount preparations and histologically, we demonstrated that they were associated with reduced amounts of prolactin in the pituitary gland and concomitantly increased levels of the hormone in the circulation. To establish whether the lactation-like phenotype was a consequence of increased circulating prolactin, we treated BTC-tg females and control littermates with bromocriptine, a potent dopamine agonist. The disappearance of the mammary gland phenotype after treatment of BTC-tg mice with bromocriptine revealed that the lactation-like changes are attributable exclusively to increased prolactin release due to a central action of BTC in the pituitary gland, instead of a local action of the growth factor in the mammary gland. Finally, by crossing BTC-tg mice to Wa5 mice carrying an antimorphic *Egfr* allele (29), we show that the changes observed in the mammary gland of BTC-tg are mediated by the EGFR instead of other ERBBs.

In a recent publication, Kansra and co-workers (24) showed in cultured GH3 lactotrophs that EGF can induce prolactin expression and release by increasing the phosphorylation of Ser-118 on the ERα in a MAPK-dependent manner. To assess whether the same pathways are responsible for the changes observed in the mammary gland of BTC-tg females, we evaluated the expression level and phosphorylation status of these molecules in their pituitary glands. While increased activation of the MAPK pathway was readily visible in the pituitary samples from BTC-tg females as compared with control littermates, no differences in the phosphorylation of Ser-104/106, Ser-118, or Ser-167 on the ERα were detectable between groups. The latter finding supports a general model in which the quite specific biological effects of the seven EGFR ligands are explained by the assembly and engagement of overlapping but distinct signaling pathways (8). In fact, it has been shown previously that EGF and BTC induce the phosphorylation of specific EGFR sites and further downstream pathways with different intensities (30). Also, overexpression of the EGFR ligand TGF-α in the mouse pituitary lactotrophs results in local hyperplasia by 6 months and adenomas that were immunopositive for prolactin at 12 months (31), while tumors have never been seen in the pituitary glands of BTC-tg mice.

At the moment, it can only be speculated about possible mechanisms involved in the BTC-induced release of prolactin. Pituitary lactotrophs are unique in having an inherent capacity for high constitutive production and release of prolactin, these processes being regulated in the form of tonic inhibition by dopamine via D2-type receptor, the predominant dopamine receptor in the pituitary lactotrophs (2, 32). Although dopamine has been recognized as the physiological inhibitor of lactotrophs for decades, its exact mechanism of action is poorly understood. Further studies will be necessary to clarify whether BTC-stimulated release of prolactin occurs by overcoming the inhibitory action of dopamine or by acting in a dopamine-independent manner.

Acknowledgments—We thank Stefanie Riesemann and Josef Millauer (Molecular Biology), Lisa Pichl (histology), Petra Renner (animal care), and Dr. Ingrid Renner-Müller (veterinary assistance).

REFERENCES

1. Bole-Feysot, C., Goffin, V., Edery, M., Binart, N., and Kelly, P. A. (1998) *Endocr. Rev.* **19,** 225–268
2. Ben-Jonathan, N., LaPensee, C. R., and LaPensee, E. W. (2008) *Endocr. Rev.* **29,** 1–41
3. Oakes, S. R., Rogers, R. L., Naylor, M. J., and Ormandy, C. J. (2008) *J. Mammary. Gland. Biol. Neoplasia* **13,** 13–28
4. Rui, H., Kirken, R. A., and Farrar, W. L. (1994) *J. Biol. Chem.* **269,** 5364–5368
5. Liu, X., Robinson, G. W., Wagner, K. U., Garrett, L., Wynshaw-Boris, A., and Hennighausen, L. (1997) *Genes Dev.* **11,** 179–186
6. Hennighausen, L., and Robinson, G. W. (2008) *Genes Dev.* **22,** 711–721
7. Yarden, Y., and Sliwkowski, M. X. (2001) *Nat. Rev. Mol. Cell Biol.* **2,** 127–137

8. Schneider, M. R., and Wolf, E. (2009) *J. Cell. Physiol.* **218,** 460–466
9. Schroeder, J. A., and Lee, D. C. (1998) *Cell Growth Differ.* **9,** 451–464
10. Vonderhaar, B. K. (1987) *J. Cell. Physiol.* **132,** 581–584
11. Kenney, N. J., Smith, G. H., Rosenberg, K., Cutler, M. L., and Dickson, R. B. (1996) *Cell Growth Differ.* **7,** 1769–1781
12. Troyer, K. L., and Lee, D. C. (2001) *J. Mammary. Gland. Biol. Neoplasia* **6,** 7–21
13. Stern, D. F. (2003) *Exp. Cell Res.* **284,** 89–98
14. Jones, F. E., Welte, T., Fu, X. Y., and Stern, D. F. (1999) *J. Cell Biol.* **147,** 77–88
15. Tidcombe, H., Jackson-Fisher, A., Mathers, K., Stern, D. F., Gassmann, M., and Golding, J. P. (2003) *Proc. Natl. Acad. Sci. U.S.A.* **100,** 8281–8286
16. Long, W., Wagner, K. U., Lloyd, K. C., Binart, N., Shillingford, J. M., Hennighausen, L., and Jones, F. E. (2003) *Development* **130,** 5257–5268
17. Luetteke, N. C., Qiu, T. H., Fenton, S. E., Troyer, K. L., Riedel, R. F., Chang, A., and Lee, D. C. (1999) *Development* **126,** 2739–2750
18. Ciarloni, L., Mallepell, S., and Brisken, C. (2007) *Proc. Natl. Acad. Sci. U.S.A.* **104,** 5455–5460
19. Finley, E. L., King, J. S., and Ramsdell, J. S. (1994) *J. Endocrinol.* **141,** 547–554
20. Fan, X., and Childs, G. V. (1995) *Endocrinology* **136,** 2284–2293
21. Murdoch, G. H., Potter, E., Nicolaisen, A. K., Evans, R. M., and Rosenfeld, M. G. (1982) *Nature* **300,** 192–194
22. Schonbrunn, A., Krasnoff, M., Westendorf, J. M., and Tashjian, A. H., Jr. (1980) *J. Cell Biol.* **85,** 786–797
23. Watters, J. J., Chun, T. Y., Kim, Y. N., Bertics, P. J., and Gorski, J. (2000) *Mol. Endocrinol.* **14,** 1872–1881
24. Ben-Jonathan, N., Chen, S., Dunckley, J. A., LaPensee, C., and Kansra, S. (2009) *Endocrinology* **150,** 795–802
25. Schneider, M. R., Dahlhoff, M., Herbach, N., Renner-Mueller, I., Dalke, C., Puk, O., Graw, J., Wanke, R., and Wolf, E. (2005) *Endocrinology* **146,** 5237–5246
26. Dahlhoff, M., Algul, H., Siveke, J. T., Lesina, M., Wanke, R., Wartmann, T., Halangk, W., Schmid, R. M., Wolf, E., and Schneider, M. R. (2010) *Gastroenterology* **138,** 1585–1594
27. Weibel, E. R. (1979) *Stereological Methods I. Practical Methods for Biological Morphometry*, Academic Press, London
28. Richert, M. M., Schwertfeger, K. L., Ryder, J. W., and Anderson, S. M. (2000) *J. Mammary. Gland. Biol. Neoplasia* **5,** 227–241
29. Lee, D., Cross, S. H., Strunk, K. E., Morgan, J. E., Bailey, C. L., Jackson, I. J., and Threadgill, D. W. (2004) *Mamm. Genome* **15,** 525–536
30. Saito, T., Okada, S., Ohshima, K., Yamada, E., Sato, M., Uehara, Y., Shimizu, H., Pessin, J. E., and Mori, M. (2004) *Endocrinology* **145,** 4232–4243
31. McAndrew, J., Paterson, A. J., Asa, S. L., McCarthy, K. J., and Kudlow, J. E. (1995) *Endocrinology* **136,** 4479–4488
32. Ben-Jonathan, N., and Hnasko, R. (2001) *Endocr. Rev.* **22,** 724–763